

Real-time observation of bond-by-bond interface formation during the oxidation of (111) Si

E.J. Adles^{1,2*}, B. Gokce^{1*}, D.E. Aspnes¹, & K. Gundogdu^{1a}

Atomic level structures of solids are typically determined by techniques such as X-ray and electron diffraction,^{1, 2, 3, 4} which are sensitive to the positions of atoms. It is hardly necessary to mention the impact that these techniques have had on almost every field of science. However, the bonds between atoms are critical for determining the overall structure. The dynamics of these bonds have been difficult to quantify. Here, we combine second-harmonic generation and the bond-charge model of nonlinear optics^{5, 6} to probe, in real time, the dynamics of bond-by-bond chemical changes during the oxidation of Si (111), a surface that has been well characterized by static methods. We thus demonstrate that our approach can provide new information about this exhaustively studied system. For example, oxidation kinetics is anisotropic even for nominally singular surfaces, with one of the three equivalent back-bonds initially reacting faster than the other two. Observed changes in bond directions show that this anisotropy leads to an initial accumulation then relaxation of strain. By comparing the bond-specific oxidation of singular and vicinal surfaces, we find that differences in surface morphology lead to different early-oxidation pathways even though the evolution of oxide thickness is unaffected. Our approach using nonlinear optics as a bond-specific characterization tool is readily adaptable for studying structural and chemical dynamics in many other condensed-matter systems.

Real-time data on the kinetics of different classes of bonds during chemical reactions can provide new insight into the reactions themselves and potentially unprecedented control over the formation of interfaces. Here, we use a combination of second-harmonic generation (SHG) and bond-charge modeling to reveal previously unresolved complexities in the oxidation kinetics of H-terminated (111)-Si, even for nominally singular surfaces. The initial oxidation is anisotropic, with changes in bond directions revealing an accumulation and later relaxation of strain.

We used p-polarization for both illumination and detection. By rotating the sample and recording the anisotropy of the SHG intensity (SHG anisotropy, or SHGA) we isolate

the contributions of individual types of bonds. Previously, nonlinear-optical anisotropy has been described using macroscopic crystal symmetry.⁷ However, during chemical changes these symmetries break and reform, making data interpretation from the macroscopic perspective challenging. We overcome this difficulty with the bond-charge model. When a bond of a particular orientation is aligned parallel to the driving field, the acceleration of that bond charge, and hence its radiated SHG signal, is maximized. This orientation dependence provides the information needed to follow chemical changes in real time on a bond-type-specific basis. We follow not only the evolution of amplitudes, for which some general data are already available,^{8, 9, 10} but also that of average bond angles and directions, which provides new information about strain. The result is a detailed picture, at the bond level, of oxidation kinetics at the Si (111) interface.

As background, the outermost atoms of the (111) surface of a tetrahedrally bonded material such as Si have one “up” orbital and three Si–Si “back” bonds. For H-passivated Si the “up” orbital is capped with H, forming a Si–H bond. On Pauling’s scale, the electronegativity of H is 2.20 while that of Si is 1.90. Hence all 4 outer-layer bonds are asymmetric: the “up” bonds from the electronegativity difference itself, and the “back” bonds from chemical induction. In a classical model this asymmetry translates into an anharmonicity of the restoring force acting on the associated bond charge, and thus the efficiency of SHG production by the charge. During initial oxidation O inserts itself into the back bonds, forming bridges between Si atoms. Since the electronegativity of O is 3.44, oxidation increases bond asymmetry and hence the SHG signal of the associated bonds.

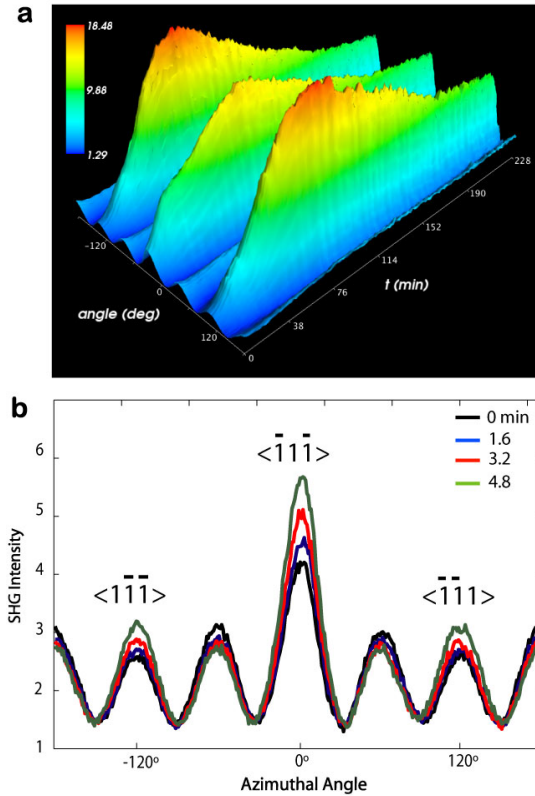


Figure 1: (a) SHGA data of an initially H-terminated singular Si(111) surface as a function of air exposure, taken at 98-second intervals. The dominant features correspond to the alignment of the $\langle -1-11 \rangle$, $\langle -11-1 \rangle$, and $\langle 1-1-1 \rangle$ bonds with the plane of incidence. The evolution of these features is discussed in the text. (b) The first four SHGA scans. The $\langle -1-1-1 \rangle$ feature rises more quickly than the other two.

Figure 1a is a three-dimensional plot of 140 consecutive SHGA scans at 98-second intervals of an on-axis, initially H-terminated sample in air. The data exhibit six features, three of which increase with time as oxidation proceeds. The dominant features correspond to the alignment of the $\langle 1-1-1 \rangle$, $\langle -11-1 \rangle$, and $\langle -1-11 \rangle$ bonds with the plane of incidence. As oxidation continues, their amplitudes reach a maximum, then decrease. The $\langle -1-1-1 \rangle$ feature rises more rapidly than the other two, indicating that the bonds along this direction are the first to oxidize. Figure 1b illustrates the initial SHG response in

more detail. The existence of anisotropic oxidation kinetics is clear: the $\langle -11-1 \rangle$ feature has reached 25% of its maximum amplitude in the first scan, and continues to rise rapidly relative to the other two. However, after 20 minutes the SHG intensity associated with the other two features rises to the level of that of the first peak. All three features reach their maximum amplitude at about 66 minutes. At later times, these amplitudes decrease, asymptotically approaching a common value. The green points in Figs. 2a–c show the evolution of the amplitudes, and illustrate these results more clearly.

The Si–O bond length of about 1.6 Å is incommensurate with the Si–Si bond length of 2.35 Å, so anisotropic oxidation is expected to introduce anisotropic strain. This strain in turn should affect the oxidation kinetics. We detect strain not only in the oxidation rates themselves, but also as changes of the widths and azimuth angles of the peaks in the SHGA data. The results are shown in Figs. 2a–c. This information was extracted by fitting the evolving SHGA features with a Gaussian function. The initial and asymptotic values have the expected equilibrium values for a Si (111) lattice, which are indicated by the dashed red lines. However, significant discrepancies are seen in the first few minutes. In particular, the $\langle 1-1-1 \rangle$ and $\langle -1-11 \rangle$ bonds both move toward smaller angles, i.e., closer to the $\langle -11-1 \rangle$ bond. Also, the $\langle -11-1 \rangle$ bond is first rapidly displaced toward $\langle -1-11 \rangle$. However, with increasing time the bonds move back toward their equilibrium positions. These changes indicate an initial accumulation, then a relaxation, of strain.

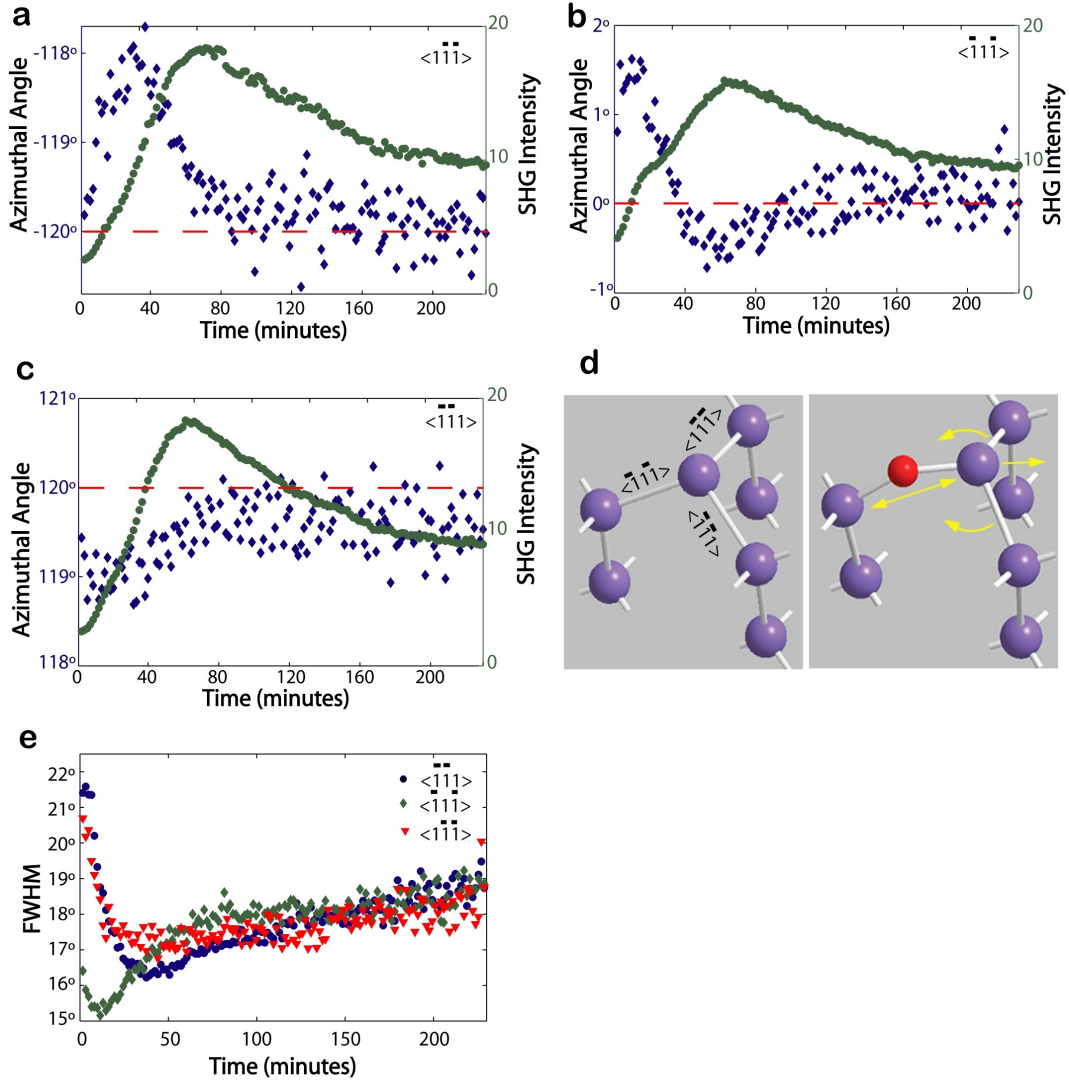


Figure 2(a,b,c) Blue points: azimuths of the three major features vs. oxidation time, obtained by a Gaussian fit. Dashed red lines: azimuths for the unperturbed crystal. Green points: corresponding amplitudes. **(d)** Atomic-scale diagram indicating expected bond distortions with an O inserted in the $\langle \bar{1}\bar{1}\bar{1} \rangle$ bond. **(e)** Evolution of the FWHM of the three main features.

The initial behavior is well reproduced by the model shown in Fig. 2d. This molecular mechanics (MM2) force-field calculation shows the result of inserting an O atom in a $\langle \bar{1}\bar{1}\bar{1} \rangle$ bond. Oxygen insertion increases the length of the bond, which in turn pushes the affected Si atoms apart. Consequently, the other two back bonds rotate in the directions observed in Figs. 2a and 2c. Nevertheless, the process is not simple, since during the return phase the angles overshoot their equilibrium positions before

asymptotically reaching equilibrium. Also, Fig. 2d suggests that the sum of the deviations of the azimuth angles of all bonds should be zero. Since this is not the case, the actual kinetics is clearly more complicated.

Additional information is obtained from the evolution of the full-width-half-maximum (FWHM) values of the major features. Figure 2e displays these for each, again extracted by the same fitting procedure. The original FWHM of all three features of the naturally oxidized surface before H termination is $16^\circ \pm 0.1^\circ$. With H-termination the relative widths bifurcate, with the FWHM of the $\langle -11-1 \rangle$ bond lower than the other two. However, during early oxidation the alignment of the bonds of a given orientation improves, as shown by the reduction in the FWHM of the peaks. The smallest FWHM values are 16.2° for $\langle -1-11 \rangle$, 17.0° for $\langle 1-1-1 \rangle$, and 15.2° for $\langle -11-1 \rangle$. Interestingly, these minima all occur when the azimuths of the associated bonds begin to return to their equilibrium positions. When each feature reaches its maximum amplitude the FWHM of each peak is about 17.5° . This, together with the continuing increase with further oxidation, suggests the onset of another randomization process. Measurements on samples 3 months after hydrogen termination indicate that the peaks continue to evolve and narrow, but at a slower pace. Thus complete relaxation back to the orientations of the ideal crystal lattice occurs on a much longer time scale. Taken together, all data indicate that oxidation follows a specific path that exhibits different kinetics for the different bond orientations.

These results are consistent across all samples of the same batch. Considering that these samples are on-axis to the best of our ability to measure them, the reason why the $\langle -11-1 \rangle$ feature is different from the other two is not obvious. On-axis Si wafers from different suppliers also exhibit anisotropy in the relative oxidation kinetics of the bonds, but the specifics differ with supplier. To the best of our knowledge this is the first report on such an anisotropy on singular Si surfaces. Whatever the cause, oxidation is highly sensitive to sample anisotropy. Since SHGA detects these anisotropies, it provides an opportunity to develop methods for interface engineering at the bond level.

To obtain further information about the dependence of oxidation on surface properties, we repeated the experiment with (111) Si wafers oriented $4.6 \pm 0.1^\circ$ toward [11-2]. Here, the surface consists of two distinct regions, steps and terraces. The terraces have the local structure of the on-axis samples. The steps have a dangling bond in the $\langle -11-1 \rangle$ direction and a support bond along $\langle -1-1-1 \rangle$, where oxidation is initiated.¹¹

Real-time SHGA data for one of these vicinal samples is shown in Fig. 3a. Six features are apparent. Three grow to approximately the same amplitude, then decay. However, the oxidation kinetics is different from that of the on-axis sample. This is highlighted in Fig. 3b, which shows the SHGA scans for the first 5 min together with those at 20 and 25 min. For the first 20 min we see little activity, and at the earliest times the $\langle -1-11 \rangle$ feature is missing. After 25 minutes the amplitudes of the major features begin to increase at a faster rate, and all reach their maximum values approximately 75 min into oxidation.

The striking difference between the on-axis and vicinal orientations indicates a strong dependence of oxidation on surface properties, particularly steps. It is known that steps facilitate oxidation of Si surfaces.¹¹ In fact the simulation shown in Fig. 3c indicates their crucial role. Here, we assume that the $\langle 111 \rangle$ support bonds at the step sides oxidize first. Then one Si-H step bond and two Si-Si* back bonds, where Si* represents a Si atom bonded to an O atom, contribute to the SHG anisotropy. The model successfully reproduces the data, indicating that for vicinal orientations oxidation indeed starts at the support bonds of the steps. Following this, oxidation of the terrace bonds dominates the SHG response.

To relate our observations to conventional oxidation studies, we also followed the evolution of both interface and SiO₂ thicknesses of these samples by spectroscopic ellipsometry (data not shown) The SE data show that the SiO₂ overlayers grow at essentially the same rate for both orientations, independent of the relatively complicated bond kinetics revealed by SHGA. Further, the maximum SHG signals are observed for both orientations when the oxide is 2–4 Å thick, which corresponds to the oxidation of the first Si bilayer. Therefore, the strain and relaxation effects that we see in the first 70 min are associated with this bilayer.

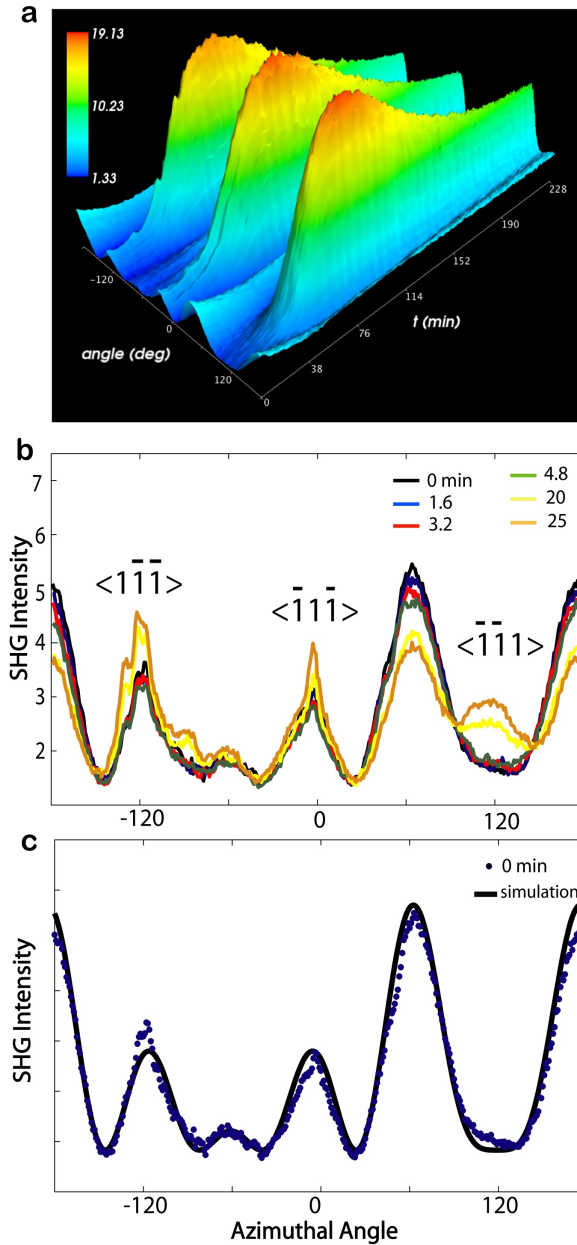


Figure 3(a) As Fig. 1, for the 4.6°-vicinal Si(111) surface. **(b)** The first four SHGA scans, together with those at 20 and 25 min. **(c)** The first SHG scan (blue dots) and simulation (black line) based on the bond-charge model, assuming that only the support bonds at the step sides are oxidized.

While structural changes in condensed matter systems have long been probed by methods such as X-ray and electron diffraction, we show here that nonlinear optics can be used to

probe analogous changes in bond structure. In the specific case studied here, we obtained information about the oxidation of Si in unprecedented detail. However, our approach is general and can be applied to problems that range from bond formation during chemical changes on surfaces to bond dynamics in functional materials that exhibit phase transitions.

Methods:

Sample Preparation: Two different sets of Si (111) samples were used in these experiments, one oriented at $0.0 \pm 0.1^\circ$ and the other at $4.6 \pm 0.1^\circ$ toward [11-2] as determined by X-ray diffraction (XRD). Each sample investigated was divided into two pieces for SHG and SE measurements. Samples were cleaned by consecutive 10-min immersions in 80 °C NaOH/H₂O₂/H₂O (1:1:5) and 80°C HCl/H₂O₂/H₂O (1:1:5). Native oxides were then stripped and the samples capped with H by a 20-min immersion in 40% NH₄F. To prevent pitting the NH₄F solution was deoxygenated prior to immersion.¹² Measurements were begun after drying the surfaces with high purity N₂, approximately 90 seconds after removal from the NH₄F. The experiments are performed under ambient laboratory conditions

References:

- 1- Rouse A. , Rischel C. , Fourmax S. , Uschmann I. , Sebban S, Grilon G. , Balcou P., Foster E. , Geindre J.P. ,Audebert P. Gauthier J.C. Hulin D. Non-thermal melting in semiconductors measured at femtosecond resolution. *Nature*, **410**, 65 (2001)
- 2- Rose-Petruck C. , Jimenez R. , Guo T. , Cavalleri A. , Siders C.W. , Raksi F. , Squier J.A. , Walker B.C. , Wilson K.R. , Barty C.P.J. Picosecond-milliangstrom lattice dynamics measured by ultrafast X-ray diffraction. *Nature*, **398**, 310 (1999)
- 3- Baum P. , Yang D.S. , Zewail A.H. 4D visualization of transitional structures in phase transformations by electron diffraction. *Science*, **318**, 788 (2007)
- 4- Siwick B.J. , Dwyer J.R. , Jordan R.E. , Miller R.J.D. An atomic-level view of melting using femtosecond electron diffraction. *Science*, **302**, 1382 (2003)
- 5- Powell, G.D. , Wang, J.F. , Aspnes, D.E. Simplified bond hyperpolarizability model of second harmonic generation. *Phys. Rev. B*, **60**, 205320 (2002)
- 6- Adles, E.J. , Aspnes, D.E. Application of the anisotropic bond model to second-harmonic generation from amorphous media. *Phys. Rev. B*, **77**, 165102 (2008)
- 7- Sipe, J.E. , Moss, D.J. , Van Driel, H.M. Phenomenological theory of optical 2nd harmonic and 3rd harmonic generation from cubic centrosymmetric crystals. *Phys. Rev. B.*, **35**, 1129 (1987)
- 8- Bergfeld, S. , Braunschweig, B. , Daum, W. Nonlinear optical spectroscopy of suboxides at oxidized Si(111) interfaces. *Phys. Rev. Lett.* **93**, 097402 (2004).

- 9- Bodlaki, D. , Borguet, E. Photoreactivity of Si(111)-H in ambient. *J. Phys. Chem. C*, **111**, 234 (2007).
- 10- Mitchell, S.A. Photooxidation of hydrogen terminated Si(111) surfaces studied by optical second harmonic generation. *J. Phys. Chem. B*, **107**, 9388 (2007)
- 11- Bensliman, F. , Sawada, Y. , Tsujino, K. , Matsumura, M. Oxidation of atomically flat and hydrogen-terminated Si(111) surfaces by hydrogen peroxide. *J. Electrochemical Society*, **154**, F102 (2007).
- 12- Wade, C.P. , Chidsey, C.E.D. Etch-pit initiation by dissolved oxygen on terraces of H-Si(111). *Appl. Phys. Lett.* **71**, 1679 (1997).

Acknowledgements

Authors thank Joshua Samberg for the X-ray diffraction measurements of the samples used in the measurements.

Author Information

¹ Physics Department, North Carolina State University, Raleigh, NC 27695-8202

² Center for Advanced Studies in Photonics Research, University of Maryland Baltimore County, Baltimore, MD, 21250

* These authors contributed equally to this work.

^a Correspondence to: K. Gundogdu¹ Correspondence and requests for materials should be addressed to K.G (Email: kgundog@ncsu.edu)